land

MDPI

Article

Composite Fingerprint Analysis of Sediment Sources in a Watershed Disturbed by Road Construction in Southeastern Tibet

Xin Li [1], Baicheng Zhu [2], Longxi Cao [2,3,*], Rui Li [2], Chunlian Bai [2] and Xinjun Wang [4]

[1] College of Earth Science, Chengdu University of Technology, Chengdu 610059, China; lixin5@cjwsjy.com.cn
[2] College of Ecology and Environment, Chengdu University of Technology, Chengdu 610059, China; 2022021048@stu.cdut.edu.cn (B.Z.); 2021021045@stu.cdut.edu.cn (R.L.); baichunlian@stu.cdut.edu.cn (C.B.)
[3] Tianfu Yongxing Laboratory, Chengdu 610213, China
[4] China Academy of Transportation Sciences, Beijing 100029, China; wangxinjun@motcats.ac.cn
* Correspondence: longxicao@cdut.edu.cn

Abstract: Construction activities such as road projects modify original land uses and intensify soil erosion. Understanding the sediment contributed by these projects and its spatial variation throughout a watershed is critical in terms of guiding conservation. Based on field sampling in a road construction-disturbed watershed in southeastern Tibet, a composite fingerprint analysis was conducted to explore the contributions of different sources to the deposited sediment. The results showed that 10 factors, including Al_2O_3, TFe_2O_3, Sn, total phosphorous (TP), Cr, Na_2O, Mn, W, SiO_2, and Sr, formed an optimum composite fingerprint combination. The multivariate mixed model revealed that the average contribution percentage rates of sediment deposited along the main channel were as follows: bank material (52.52%) > roads (33.02%) > forest and grassland (14.46%). The contribution percentage of road-related sediment fluctuated from the beginning point along the channel and was significantly correlated with factors such as the flow length to the channel (R = −0.6), road segment slope (R = 0.66), and ratio of the road length to the channel length (R = 0.65). The flow length to the channel was the most important factor affecting the road sediment contribution and a decreasing logarithmic function was established to describe the effect. These results have clarified how road construction spatially affects sediment at the watershed scale. They can therefore offer guidance for evaluating the environmental impact of human activities and supporting efforts in watershed soil and water conservation.

Keywords: composite fingerprint; road construction; sediment sources; Southeast Tibet

check for updates

Citation: Li, X.; Zhu, B.; Cao, L.; Li, R.; Bai, C.; Wang, X. Composite Fingerprint Analysis of Sediment Sources in a Watershed Disturbed by Road Construction in Southeastern Tibet. *Land* **2024**, *13*, 929. https://doi.org/10.3390/land13070929

Academic Editor: Wojciech Zgłobicki

Received: 6 May 2024
Revised: 5 June 2024
Accepted: 22 June 2024
Published: 26 June 2024

Copyright: © 2024 by the authors. Licensee MDPI, Basel, Switzerland. This article is an open access article distributed under the terms and conditions of the Creative Commons Attribution (CC BY) license (https://creativecommons.org/licenses/by/4.0/).

1. Introduction

Human activities are the primary factors that accelerate global soil erosion by changing land use [1]. As society progresses and economies expand, soil erosion caused by construction disturbances is increasingly a concern of scientists [2–4]. Among these disturbances, the construction of various types of roads has been identified as one of the main causes of soil erosion, and this phenomenon has been reported worldwide in the last few decades [5]. Road-related construction activities, such as excavation and filling, can directly damage surface soils and vegetation, thereby exacerbating the risk of soil erosion [6,7]. Eroded sediment from disturbed areas can enter nearby water bodies and cause severe damage to aquatic environments [8,9]. Furthermore, sediment deposition within channels can result in the silting of river reservoirs, which compromises their ability to control flooding and store water, thereby increasing the likelihood of floods [10–13]. Therefore, an accurate assessment of sediment generation due to road-related soil erosion in watersheds is crucial for construction planning and developing conservation practices.

Traditional methods for identifying sediment sources typically rely on feature analysis of hydrological and erosion factors, and these methods are known for being time-consuming

and resource-intensive. In recent decades, composite fingerprinting techniques have become increasingly popular for investigating sediment sources within watersheds [14]. Composite fingerprinting involves evaluating erosion source contributions by comparing the chemical, physical, biological, or magnetic characteristics of sediment with those of potential sources [14,15]. This approach has been used extensively in regions undergoing significant soil and water loss, such as the UK [16,17], the US [18,19], Iran [20,21], and different regions of China [22–26]. Scientists have quantified the sediment contributed by engineering activities, such as road networks, and have established that road construction has a significant impact on soil erosion and sedimentation in watersheds [15,27,28]. In most cases, recent research on watershed-scale road sediment contributions has been conducted by examining the deposited or suspended sediment present at watershed outlets. Investigations of the spatial variations in road-related sediment contributions at different catchment-scale positions are rare. Considering the linear road networks that extend across a watershed, the spatial variability of sediment associated with roads in adjacent channels is critical for guiding conservation efforts [29]. This is especially important for watersheds that are ecologically fragile.

The region downstream of the Yarlung Tsangpo River Basin (YTRB) in southeastern Tibet is distinguishable by its primitive ecosystems and thus serves as a crucial regional ecological barrier [30]. However, rapid increases in human activity and engineering disturbances, such as road construction, have significantly altered local land use and sediment generation [31]. Soil and water loss due to these disturbances are of paramount concern, as they pose a significant threat to the aquatic environment in the watershed [32]. A comprehensive and quantifiable analysis of the impact of disturbances by engineering activities on erosion and sedimentation is therefore required to protect the aquatic environment in the area. Shi et al. (2018) [33] observed spatiotemporal variations in suspended sediment transport in the Yarlung Tsangpo River and reported that the sediment contribution was lower than that of other rivers originating on the plateau. However, Li et al. (2024) [34] reported that 30% of the total suspended sediment flux was deposited within rivers on the Tibetan Plateau; thus, the magnitude of the erosion might be underestimated. Using soil erosion models, such as the revised universal soil loss equation (RUSLE) model, scientists have evaluated the risk of soil erosion in the YTRB and discussed potential hazards caused by sediment transported to rivers [35,36]. The composite fingerprinting technique has also been used for an agro-pastoral watershed assessment of this region, and the results showed that farmland contributes 50% of the suspended sediment [30]. Huang et al. (2020) [31] investigated the response of the suspended sediment flux to human activities in a tributary of the YTRB and reported that road construction sharply increased the suspended sediment concentration in the surveyed river. The above studies have revealed trends of total sediment generation and highlighted the significant impacts of infrastructure projects, such as road construction, in the YTRB. Nevertheless, specific spatial identification of road-related sediment contributions at the watershed scale, which is vital for conservation programs, is still lacking.

This study aims to fill the identified knowledge gap by examining a typical watershed impacted by road construction. By utilizing the composite fingerprint method, our research seeks to accomplish two main goals: (1) identifying sediment contributions from areas of road construction disturbances compared with those from other land use types and (2) revealing the spatial variation in road-related sediment contributions and clarifying the driving mechanisms. By enhancing the understanding of how road construction spatially affects sediment in the watershed in the study area, this study can broaden the applicability of the composite fingerprint method. Additionally, the results can assist in environmental assessment and optimization of soil and water conservation measures within the YTRB.

2. Materials and Methods

2.1. Study Area

The study area is the Doxiong River watershed in southeastern Tibet; the Doxiong River acts as a secondary tributary of the Yarlung Tsangpo River (Figure 1a). Extending from longitudes 94°50′ to 95°12′ E and latitudes 29°33′ to 29°19′ N, the watershed encompasses an area of 146.2 km^2. The watershed exhibits a long, narrow canyon-type configuration running northwest to southeast, characterized by elevations ranging from 1178 m to 5413 m, thereby fostering diverse climatic conditions. The areas with elevations exceeding 3000 m are marked by a mountainous cold temperate climate, featuring an average annual air temperature of 5 °C. The vegetation is dominated by cold temperate coniferous forests, while the primary soil types include black felt soil and cold tundra (Leptosols according to the World Reference Base (WRB) system). Conversely, the areas below 3000 m have a predominantly subtropical and humid climate characterized by an average annual temperature of 14 °C and an annual precipitation reaching 2200 mm. The vegetation is dominated by subtropical broad-leaved evergreen forests, while the primary soil types consist of dark brown soil and dark yellow-brown soil (Luvisols according to the WRB system). The land within the watershed is predominantly forested, encompassing an area of 69.68 km^2. Bare rock (34.78 km^2) is mainly found above an elevation of 3000 m, and grasslands and shrubs cover an area of 34 km^2. Generally, the forested areas exhibit minimal risk of erosion due to their extensive coverage (Figure 1b). In some cases, grazing activities in grassland zones may lead to soil loss (Figure 1c). Notably, some channels suffer intensive erosion due to the accumulation of water upstream. This kind of erosion sometimes also involves debris flow trenches or gullies (Figure 1d).

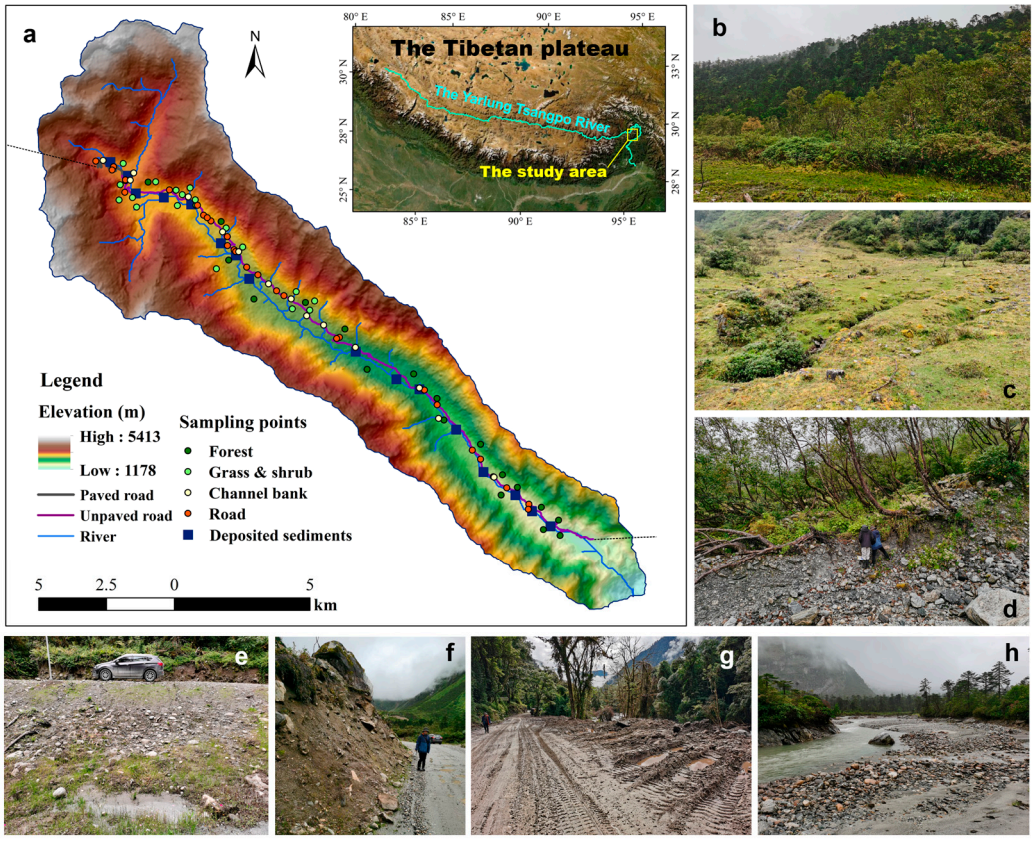


Figure 1. Study area and sampling points. (**a**) The location of the study area and the sampling points; (**b**–**d**) photos of a forest, grassland, and channel bank, respectively; (**e**–**g**) photos of the eroded road embankment, cutslope, and the disturbed road surface, respectively; (**h**) one of the deposited sediment sampling sites.

The main infrastructure project affecting the studied watershed is the G219 National Highway, which spans 30.8 km within the Doxiong River watershed and is predominantly situated below 3000 m above sea level. Beginning at the northern bank of the Doxiong River, the highway traverses various subwatersheds along its route. It passes through complex topography and exhibits an elevation difference of 1660 m between its starting and ending points. The construction of the highway span in the Doxiong River watershed occurred from November 2018 to November 2020. After completing the road embankment, most of the road remained unpaved throughout 2021, except for a small span (about 2.5 km long) near the starting point, which was paved. At this stage, construction efforts were focused on the tunnel on the southeast side of the Doxiong River watershed, with no further work on the road embankment. Therefore, the highway should be treated as an unpaved road, with the road surface generally consistent throughout the watershed. Additionally, highway construction has disrupted the natural terrain, resulting in engineering cutslopes (average slope = 42.6°) and fillslopes (average slope = 38.4°) (Figure 1e,f). Most of these slopes have been treated with simple conservation measures, such as sowing grass seed to create sparse ground cover, but soil erosion remains intense, with rill erosion frequently observed (Figure 1e). A road drainage system consisting of ditches and culverts has been constructed to allow the overland flow to pass through. Given the general alignment of the highway parallel to the Doxiong River, an influx of sediment into the river is inevitable, which negatively impacts the aquatic environment.

2.2. Field Sampling and Road Survey

According to the research of Shi et al. (2018) [33], sediment transport or deposition within watersheds in the study area mainly occurs from July to September. Therefore, fieldwork was conducted in late September 2021 to collect soil and sediment samples, including surface soil samples from potential sediment sources and sediment samples from deposits along the primary channel in the watershed. Surface soils were primarily sampled from the abovementioned sediment sources, including roads, channel banks and gullies, natural forests, and grasslands. It is important to note that bare rock areas were generally excluded when assessing soil erosion on the Tibetan Plateau [37] and were therefore not considered as potential sediment sources. In natural forest and grassland areas, sample sites were selected on relatively gentle slopes representative of the type of vegetation coverage. For each sampling site, three subsamples were collected within a 2×2 m^2 area. The litter layer was removed to collect the top layer (0–5 cm) samples of the mineral soil. For channel bank sources, sampling sites were chosen in tributaries or gullies along the main channel. Samples were taken by collecting the surface layer of 2 cm thickness from the sidewall of channel bank. Three replicates would be collected to form a composite sample. For road-related sources, road surface sites were selected in areas where significant erosion was evident. Topsoil samples (0–2 cm) were taken along the transverse line of the road surface. Sampling for cutslope sources was similar to those for channel banks and gullies, with a 2 cm surface layer collected. On fillslopes, the soil is relatively loose and therefore 0–5 cm of topsoil was sampled to reflect the depth of rill erosion. All road-related samples were composite samples, each consisting of three subsamples per site. During sampling, visible soil blocks and other contaminants were removed before the samples were bagged for further analysis. Each sample weighed approximately 1 kg, and a total of 98 samples were collected: 18 from forested areas, 20 from grasslands and shrub lands, 30 from unsealed road surfaces and roadside slopes, and 14 from channel banks.

This study investigated sediment deposition at different locations along the main channel to evaluate the contributions of sediment from sources within the catchment. Sixteen sediment sampling sites were chosen based on the watershed elevation, drainage conditions, and sediment source distribution. The sampling sites were located along the main channel, covering a total length of 24.68 km. Eight sites were located in the upper watershed, predominantly above 3000 m, covering a channel distance of 8.62 km. The remaining 8 sites were situated in the lower portion of the watershed, below 3000 m,

covering a channel distance of 10.66 km. Each of the sediment sampling sites was located where significant deposition had occurred within the main channel. For example, in the lower part of the tributaries at the confluence point, the channel gradient becomes gentle, or the riverbed widens. The above reason for choosing the sampling sites ensures that one sampling site represents the sediment transport process within the area between it and the adjacent upstream site [36]. Multipoint mixed sampling was conducted at each site and the surficial samples were collected to reflect the recently deposited sediments [38]. Mixed sediment samples weighing approximately 1 kg were stored in bags for subsequent analysis.

A field survey was also conducted to measure road undulations and interactions with channels. The specific locations of the high points, low points, and culverts along the road were recorded. Then, the road was divided into 178 different segments. Each of the road segments was defined by two adjacent high and low endpoints that divided the flow and therefore could be treated as the basic units in which soil erosion and sediment generation occurred. These segments were summarized to fit the 16 sediment sampling sites and to calculate influential factors. Factors that may affect sediment generated by roads and transport to channels were selected according to Elliot et al. (2004) [39]. Table 1 shows the implications of different factors and the methods used to acquire the factors. The terrain data adopted in this study are from the 12.5 m Advanced Land Observing Satellite (ALOS) Digital Elevation Model (DEM) (https://search.asf.alaska.edu/ (accessed on 2 May 2024)), and spatial and hydrological analyses were conducted in ArcGIS 10.3.

Table 1. Factors influencing sediment contributed by roads.

Abbreviation	Name	Calculation Method
CL	Channel length	Horizontal channel length between two adjacent sampling sites
RL	Road length	Horizontal road segment length between two adjacent sampling sites in the channel
R/C	Ratio of the road length to the channel length	Road segment length divided by the channel length at a point above the same sampling site
CS	Channel gradient	Elevation difference between two adjacent channel sites divided by the channel length
RS	Average road segment gradient	Elevation difference between the high point and low point divided by the road segment length
CRD	Average distance from the river to the road	Average Euclidean distance between the road and channel within the area between two adjacent sampling sites
CRS	Average slope between the river and the road	Average hillslope gradient between the road and channel within the area between two adjacent sampling sites
FL	Flow length	Flow length between one sampling site and the nearest road culvert
FLS	Slope gradient along the flow length	Elevation difference divided by the flow length

2.3. Laboratory Analysis

In this study, soil samples were collected to obtain soil indicator data. The samples were air dried and then processed using a freeze dryer. They were subsequently ground and sieved to 2 mm before being further processed to achieve a size of <63 μm for index testing (Figure 2), as the <63 μm fraction is arguably the most commonly used particle size fraction for sediment tracing [40]. To identify sediment indicators, 18 physical and chemical soil indices were selected. These methods were based on the geological and chemical background of the study area, as well as previously used composite fingerprinting methods [41]. The soil indicators were determined by different methods: Na_2O, MgO, Al_2O_3, SiO_2, K_2O, and CaO were measured via plasma emission spectrophotometry, while Mn, Zn, Cu, Cr, Co, Sn, Sr, Ni, and TFe_2O_3 were determined using X-ray fluorescence spectrophotometry. The total phosphorus (TP) content was quantified using molybdenum

blue extraction ultraviolet spectrophotometry, and the total nitrogen (TN) content was determined via high-temperature decomposition using an automatic tester. Finally, soil organic carbon (SOC) was analyzed via the potassium permanganate oxidation method.

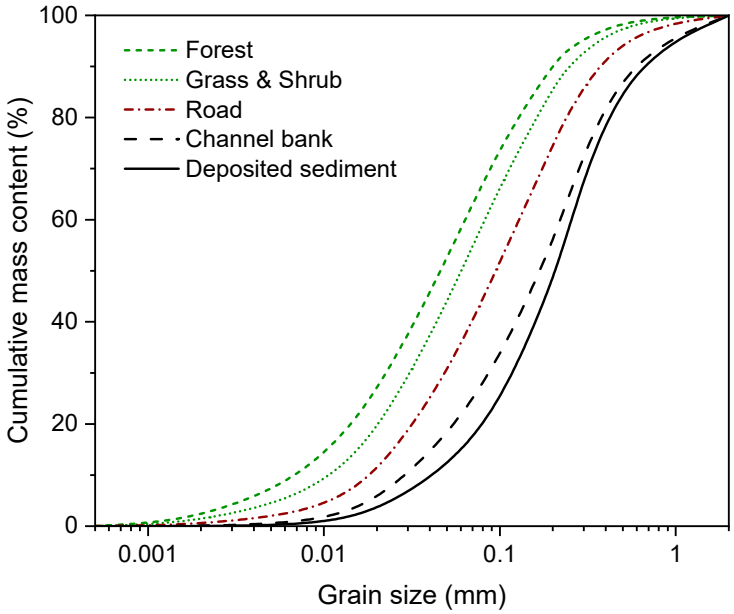


Figure 2. The grain size curves of different sources and sediment samples.

2.4. Selection of Composite Fingerprints

Considering the studied watershed is relatively small and the channel structure is simple, we used all source samples to represent the fingerprints of the whole catchment. The application of sediment fingerprinting techniques is based on the assumptions that tracers follow conservatism and that the selected tracers behave conservatively during movement and migration within the catchment [14]. There is a direct link between the source and the sediment through the tracer; therefore, before applying the fingerprinting technique, a conservatism test should be carried out to select a tracer with conservative behavior. A commonly used conservatism test is the range test: (1) the range of tracer concentrations in all sediment samples must be within the range of all source samples; (2) the average tracer concentration in all sediment samples must be within the range of the average source sample concentration [42]. The composite fingerprinting technique, as outlined by Collins et al. (1997) [43], consists of two steps: first, the nonparametric Kruskal-Wallis H test is employed to identify potential fingerprint recognition factors; second, multivariate stepwise discriminant analysis (discriminant function analysis, DFA) is utilized to determine the optimal combination of fingerprint factors. The Kruskal-Wallis H test, a test for ranking data from multiple population samples, is suitable for comparing samples with completely randomized groupings. Significant differences in the overall distribution of each sample group are indicated if intergroup differences can explain the overall rank difference across multiple sample groups; otherwise, the overall difference in the distribution is deemed insignificant. The null hypothesis posits that all sediments originate from a single source. A comparison of the H value of the test statistic with the chi-square test result (Hcr) enables the null hypothesis to be rejected (H > Hcr), indicating the factor's ability to differentiate the sediment source [44,45], as illustrated in Equation (1).

$$H_{calc} = \frac{12}{N(N+1)}\left(\sum_{s=1}^{n}\frac{R_S^2}{n_1}\right) - 3(N+1) \quad (1)$$

In Equation (1), R_S represents the rank of source location S, n_1 represents the number of samples taken from source location S, and N represents the total number of sediment

samples collected at the source location. The p value is the significance probability, and a value of $p < 0.05$ suggests attribute H > Hcr, implying a significant difference between the groups regarding that attribute, making it a potential fingerprint factor. Factors that do not demonstrate significant differences, as indicated by $p > 0.05$, were removed from further consideration.

The composite fingerprint was generated by using multivariate stepwise discriminant analysis (DFA) on potential fingerprint factors following the Kruskal-Wallis H test results. The Wilks' lambda formula was utilized as the primary discriminant criterion in stepwise discriminant analysis to identify variables with intergroup discriminating power and to select multiple variables for the investigation. When the mean values of the observation groups are equal, the Wilks' lambda value is 1, whereas the Wilks' lambda value approaches 0 when the within-group variation is relatively small compared to the total variation [44,45]. Multivariate discriminant analysis was used to identify the group of fingerprint factors with the smallest Wilks' lambda value as the most discriminatory composite fingerprint factor, and the Wilks' lambda (Λ) was calculated as follows (2):

$$\Lambda = |SS\text{error}|/|SS\text{error} + SS\text{treat}| \quad (2)$$

where SSerror is the sum of squares of deviations within the group and SStreat is the sum of squares of deviations between groups.

2.5. Apportionment of Sediment Sources

The optimal fingerprint combination was determined using multivariate stepwise discriminant analysis. Additionally, a multivariate mixed model was employed to evaluate the sediment contributed by each source. Currently, the Walling model is the prevailing mixed model, with the minimum value of the target function representing the proportion of sediment from the source. Its mathematical representation is outlined below [46]:

$$Res = \sum_{i=1}^{n} \left\{ \frac{C_{ssi} - (\sum_{s=1}^{m} C_{si} P_s)}{C_{ssi}} \right\}^2 \quad (3)$$

In the equation, Res represents the residual sum of squares, C_{ssi} represents the concentration of sediment in the study area defined by the fingerprint factor,P_s represents the percentage of sediment contributed from source s, C_{si} denotes the average concentration of sediment in the source area defined by the fingerprint factor s, m represents the number of sediment sources, and n represents the number of fingerprint recognition factors.

The mixed model operates based on two implicit conditions. First, the total contributions from the different sources must add up to 1. Second, the contributions from each source must not be negative. To evaluate the fit between the results of the mixed model and the observations, the model proposed by Collins et al. (2010) [2] was used.

$$\text{GOF} = 1 - \frac{1}{n} \times \sum_{i=1}^{n} \left\{ \frac{C_{ssi} - (\sum_{s=1}^{m} C_{si} P_s)}{C_{ssi}} \right\}^2 \quad (4)$$

In general, the optimized results from the mixed model calculations are considered valid only if the goodness of fit (GOF) exceeds 0.8.

2.6. Statistical Analysis

In this study, Pearson correlation analysis and regression analysis were adopted to quantify the relationships between road sediment contribution rate and its influential factors. Moreover, the importance ranking of random forest feature variables was also adopted to quantify the contributions of influential factors to the rate of sediment contributed by the road. The steps in this method are to calculate how much each feature contributes in each decision tree within the random forest, average the results, and then compare

the size of the contribution between features. The random forest algorithm estimates the contribution of the target variable by measuring the extent to which the predicted error increases when the out-of-bag (OOB) data of the target variable are rearranged while all other data are held constant [47]. In this study, the relative importance of each impact factor to the rate of sediment contributed by the road was quantified using the importance ranking of characteristic random forest variables in Spyder, and the calculated results were normalized. All graphics were generated with the ORIGIN 2022 software package (OriginLab, Northampton, MA, USA).

3. Results

3.1. Selecting the Composite Source Fingerprint

Figure 3 shows that SiO_2, K_2O, Na_2O, CaO, MgO, Al_2O_3, TFe_2O_3, Mn, Sn, Sr, Co, Cu, W, and TP exhibited a uniform pattern of variations among the four source types and the deposited sediment. The concentrations of the above parameters in road sediment, bank materials and deposited sediment were notably greater than those in natural forest and grassland soils. Conversely, soil organic nutrient levels (SOC and TN) were significantly greater in natural forest and grassland soils than in the other three materials. Figure 3 also shows that the minimum SOC (0.81 g/kg) and TN (0.03 g/kg) levels in the deposited sediments were lower than those in the source area sediments (1.64 g/kg and 0.08 g/kg for SOC and TN, respectively) and were therefore excluded from further analysis due to their lack of conservative characteristics. The remaining factors were subjected to nonparametric Kruskal-Wallis H tests.

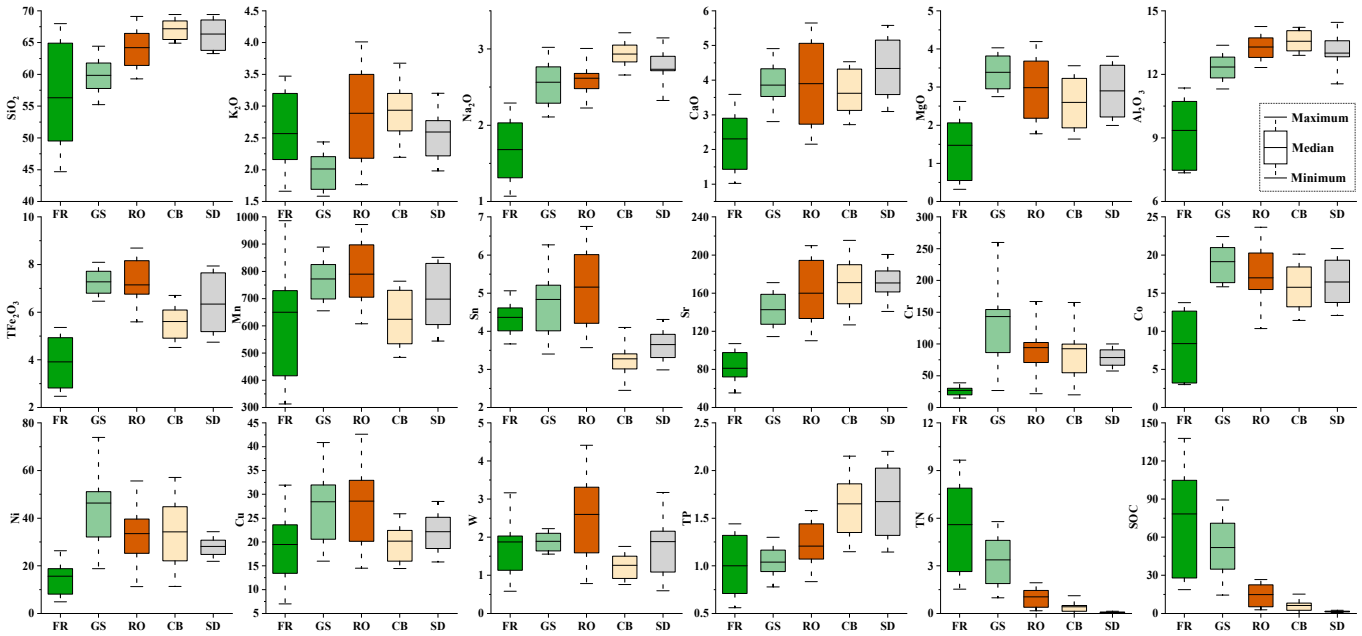


Figure 3. Box plot of concentrations of parameters in sediments from different erosion sources and riverbeds. FR, GS, RO, CB and SD stand for forest, grassland, road, channel bank and deposited sediment, respectively.

Table 2 shows the results, which indicate that 16 factors exhibited statistical significance ($p < 0.01$), showing significant differences in concentrations between the groups and an effective ability to discriminate, thus passing the test. It should be mentioned that the distinction between the road and the grassland and shrubland sources is not pronounced. This may be partly due to the fact that the road passes through grassland and shrubland areas. Additionally, the vegetation restoration measures carried out on the roadside slopes may also contribute to the insignificant differences in the indices between the road and grassland sources. Multivariate stepwise discriminant analysis (DFA) was then performed.

Table 3 and Figure 4 show the findings of a linear discriminant analysis, with a linear discriminant (LD) 1 value of 56.14% and an LD 2 value of 36.54%. The results reveal that the optimal combination of fingerprint factors is Al_2O_3, TFe_2O_3, Sn, TP, Cr, Na_2O, Mn, W, SiO_2, and Sr. Using these factors, an overall correct classification rate of 92.66% for the source area is achieved. The results demonstrate that the selected combination of fingerprint factors achieves high accuracy in distinguishing different source areas. Therefore, the optimal combination of fingerprint factors for measuring the sediment contribution from source areas to sediment deposited in the main channels in the study area is determined.

Table 2. Results of the nonparametric Kruskal-Wallis H test on the fingerprint properties of the source type.

Potential Identifiers	H-Value	*p* Value	Potential Identifiers	H-Value	*p* Value
SiO_2	28.73	0.000	Sn	27.48	0.000
K_2O	21.32	0.000	Sr	39.26	0.000
Na_2O	42.29	0.000	Cr	37.87	0.000
CaO	18.61	0.000	Co	36.23	0.000
MgO	29.31	0.000	Ni	28.69	0.000
Al_2O_3	51.94	0.000	Cu	17.21	0.001
TFe_2O_3	46.87	0.000	W	21.95	0.000
Mn	16.23	0.001	TP	16.17	0.001

Table 3. Optimal composite fingerprint for discriminating sediment source types.

Step	Fingerprint Property Selected	Wilks' Lambda	Source Types Classified Correctly
1	Al_2O_3	0.288	55.83
2	TFe_2O_3	0.158	73.14
3	Sn	0.094	79.74
4	TP	0.073	81.83
5	Cr	0.058	81.83
6	Na_2O	0.047	82.91
7	Mn	0.040	83.08
8	W	0.035	85.16
9	SiO_2	0.031	86.60
10	Sr	0.027	92.66

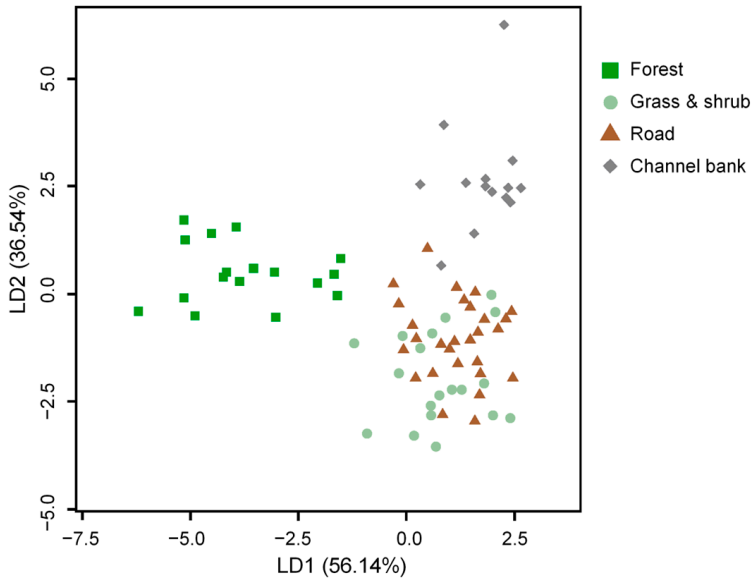


Figure 4. Linear discriminant analysis.

3.2. Contribution from Sediment Sources

The relative contributions from erosion sources to the sediment deposited at the different sites were determined based on the optimal fingerprint factors and the Walling-Collins multivariate linear mixing model. The results in Table 4 indicate that channel bank-related sediment accounts for the highest average percentage of sediment contributed (52.52%) to the deposited sediment, followed by roads (33.02%), grasslands (8.29%), and forests (6.17%). The goodness of fit (GOF) values of the calculated results of the contributed sediment have a range of 0.942–0.988 and an average of 0.963, and all GOF values are greater than 0.8, thereby indicating the acceptability of the results.

Table 4. Sediment contributions from the different sources.

Sediment Site	Relative Rates of Sediment Contributed by Different Sources/%				*Res*	GOF
	Forest	Grass	Road	Bank		
S1	3.73%	10.01%	84.15%	2.11%	0.376	0.962
S2	2.64%	13.53%	1.21%	82.62%	0.580	0.942
S3	2.13%	8.05%	73.93%	15.88%	0.350	0.965
S4	3.88%	5.65%	2.18%	88.29%	0.437	0.956
S5	1.71%	7.12%	42.03%	49.14%	0.398	0.960
S6	2.35%	1.34%	33.29%	63.02%	0.456	0.954
S7	2.62%	1.61%	20.56%	75.21%	0.545	0.945
S8	1.07%	28.52%	4.33%	66.08%	0.468	0.953
S9	3.64%	2.90%	22.42%	71.03%	0.441	0.956
S10	5.42%	16.32%	38.11%	40.16%	0.329	0.967
S11	1.65%	29.22%	1.42%	67.71%	0.392	0.961
S12	39.32%	1.12%	38.37%	21.19%	0.220	0.978
S13	1.82%	2.43%	73.40%	22.35%	0.297	0.970
S14	21.32%	2.68%	3.90%	72.10%	0.405	0.959
S15	3.18%	1.12%	52.56%	43.14%	0.122	0.988
S16	2.18%	1.03%	36.41%	60.38%	0.161	0.984
AVE	6.17%	8.29%	33.02%	52.52%	0.374	0.963

As shown in Table 4, there is great variability in the sediment composition among the different sites. To further reveal the spatial variation in the rates of contributed sediment along the main channel, the sediment site data were overlain by land use data at the watershed scale (Figure 5). The average rates of contributed sediment for the upper and lower parts of the watershed are generally consistent. There is a slight decrease (from 55.3% to 49.8%) in the amount of bank-related sediment with the decreasing number of tributaries from the upper to the lower part of the watershed. On the other hand, the average sediment contribution from forest sources increases from 2.5% to 9.8% with the increasing forest area when comparing the upper and lower parts. The road-related sediment showed similar average rates of contribution between sites from both parts of the watershed. At the most upstream sediment site (S1), road segments that zigzagged close to the river contribute more than 80% of the channel sediment. Then, the rate of sediment contributed by the road generally decreases from S2 to S8 as the road moves relatively far from the main channel, except for the high contribution rate of S3, which is located at the intersection of the road and the river. Conversely, S2 and S4, which were connected to low-gradient road segments, showed little road sediment contribution. In the lower part of the watershed, where the valley becomes narrow and the road is generally close to the channel, the rate of contributed sediment increases from S9 to S16. The two natural land use types show different changes from the upper to the lower part of the watershed. The rates of contributed sediment from the forestland are less than 5% for sites S1 to S9 but increase along the lower part of the main channel from S10 to S16. On the other hand, the rates of contributed sediment from the grassland are relatively high from S1 to S11, within which grassland is distributed along both sides of the main channel. With decreasing grassland area, the rates of sediment

contributed by this kind of sediment source are very low (less than 3%) from S12 to S16. Generally, the rates of sediment contributed by both forests and grasslands account for less than 20% of the total sediment, except at 5 sites from section S7 to S14. As the highest sediment source in the watershed, bank-related sediment accounts for more than 50% of the total sediment at most of the sites (9 out of 16). The rate is especially high (more than 80%) at the confluence of two major tributaries (S2 and S4).

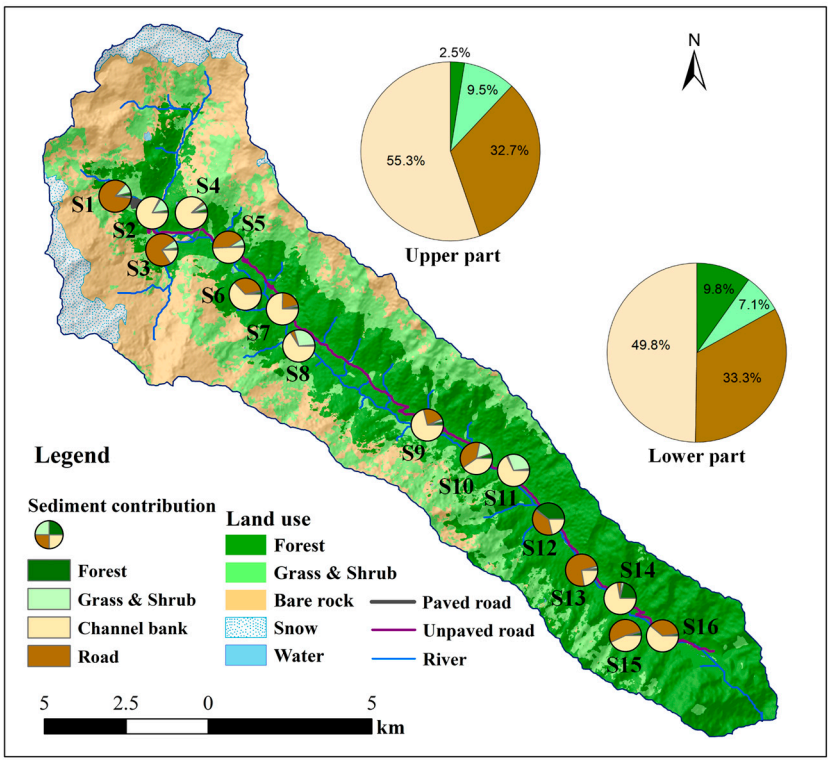


Figure 5. Spatial distribution of sediment contributed by different sources.

3.3. Factors That Influence Road-Related Sediment Contributions

To analyze the factors influencing sediment contributed by roads, nine factors described in Table 1 were calculated and correlated with the rates of sediment contributed by the roads at the 16 sampling sites (Figure 6a). Four factors have significant relationships with the rate of sediment contributed by the road. The positive correlation between the ratio of the road length to the channel length (R/S) and the road rate of contributed sediment is statistically significant (R = 0.65) compared with that between both the channel length and road length, which shows relatively small correlation coefficients. The slope gradient also has an important effect on the rate of sediment contributed by the road. Both the channel gradient and the average road segment gradient are positively correlated with the rate of sediment contributed by the road (R = 0.54 and 0.66 for CS and RS, respectively). Similarly, the average slope gradient between the road segment and channel (CRS) and the gradient along the flow route between the road and sampling site (FLS) are also positively correlated with the rate of sediment contributed by the road, although the correlation coefficient is not significant (R = 0.31 and 0.19 for CRS and FLS, respectively). On the other hand, factors that reflect the distance from roads to channels are negatively related to the rate of sediment contributed by the road. The flow length between the sampling sites and the road culvert (FL) show a significant correlation coefficient (R = −0.60). The average distance between roads and channels (CRD) is also negatively related to the rate of sediment contributed by the road, with a nonsignificant correlation (R = −0.27).

Figure 6b shows the ranked results of the random forest feature importance. The flow length (FL) is the most important factor (0.211), followed by the CRD (0.151), road length (RL) (0.148), R/C (0.139), RS (0.133), and CS (0.108), with importance values greater than 0.1.

On the other hand, three factors, CL, FLS, and CRS, show relatively low importance. Further regression analysis was conducted to explore the relationships between the four significant impact factors and the rate of sediment contributed by the road (Figure 7). Linear equations can be established to describe the effects of the channel gradient, slope gradient of the road segment, and the ratio of the road length to the channel length. The contribution rates of sediment from the roads to the different sampling sites increase linearly with these factors. On the other hand, a logarithmic function was built to quantify the negative relationship between flow length and the rate of sediment contributed by the road. The proportion of road-related sediment seems to decrease with flow length when it is transported out of the road areas to nearby downstream channels.

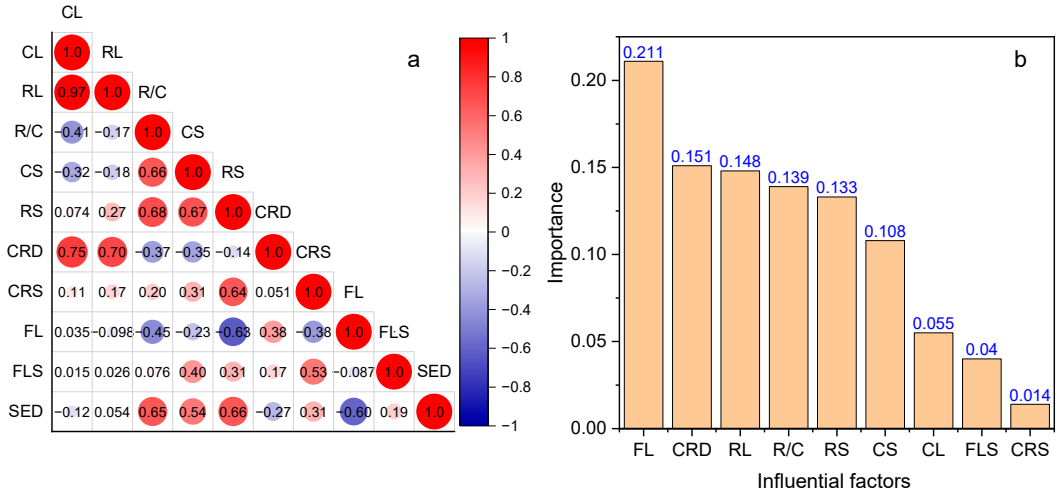


Figure 6. Correlation coefficients (**a**) and the importance (**b**) of influential factors in affecting rates of sediment contributed by the roads. The abbreviations of influential factors are explained in Table 1. SED stands for the rate of sediment contributed by the road.

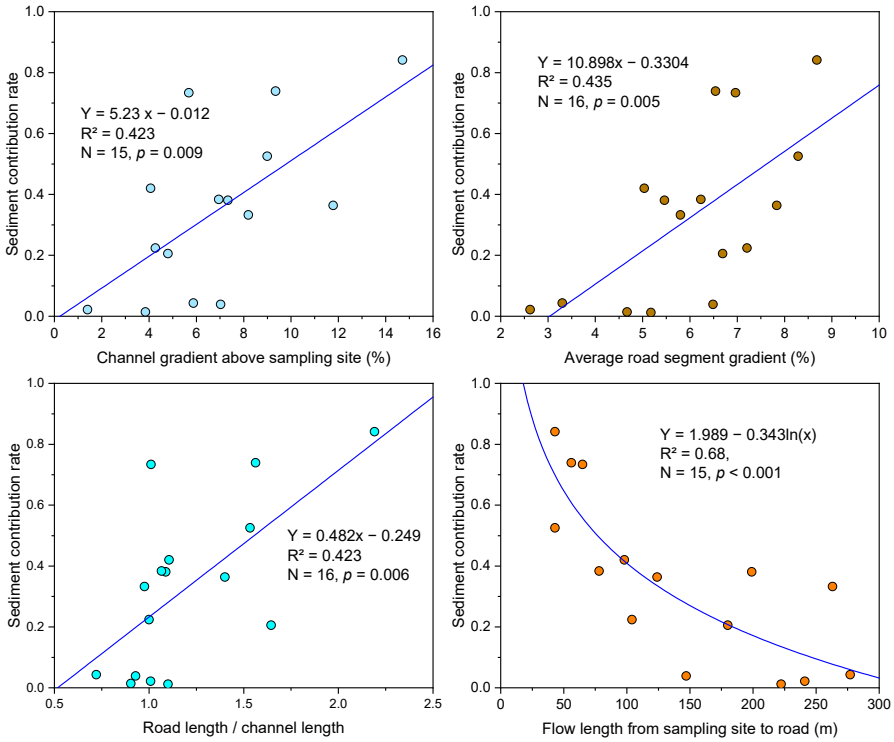


Figure 7. Rate of sediment contributed by the road as a function of different factors. Note: one site has been removed to build a better equation with channel gradient or flow length.

4. Discussion

4.1. Contribution of Road-Related Sediment

In the Doxiong River watershed, both forest and grassland, which account for more than 70% of the total area, contributed only 14.46% of the sediment deposited along the sampled channel. The low sediment contributions from forest and grassland reflected the high coverage and soil erosion resistance of the hillslopes protected by natural vegetation. This result is in accordance with Chen et al. (2023) [35], who reported that the background soil erosion of hillslopes in the study area is mainly slight (<5 t/ha/a) or light (5–25 t/ha/a). On the other hand, the highest rate of contributed sediment for the bank sediment implies the influence of weathered materials, which have been reported as one of the primary sediment sources in the YTRB [33]. Notably, road-related sediment accounted for an average percentage of 33.02% at the different sampling sites along the main channel, although the total road surface area only accounted for approximately 0.21% of the watershed area (0.3 km^2). This reflected the effect of disturbance by road construction on soil erosion and sediment generation. Similarly, Huang et al. (2020) [31] reported an approximately four-fold increase in the suspended sediment concentration due to road construction in a tributary watershed of the YTRB. Thomaz et al. (2014) [48] also noted that the suspended sediment concentrations downstream of stream crossings were between 3.5 and 10 times greater than that upstream. Our contribution rate is greater than that of Farias et al. (2021) [49], who reported that roads, which occupy 0.7% of the catchment surface, were responsible for approximately 7% of the soil loss in the area.

As most of the highway span within the Doxiong River watershed was unpaved during our study period, the compacted road surface is characterized by low infiltration and high runoff generation capacity [50]. This would increase runoff and lead to a higher risk of soil erosion on the unpaved road surface [51]. Additionally, heavy vehicles passing through for construction activities disturbed the unpaved road surface, resulting in highly erodible material (Figure 1g) [52], thus accelerating the soil erosion process. The road cutslopes also suffer from soil erosion due to intercepted upstream runoff and gravitational erosion [53,54]. Besides the abovementioned sediment source perspectives, the road drainage system of ditches and culverts would increase the sediment connectivity between the road and the river. This in turn would allow more sediment from road-related sources to be transported to the nearby channel [55]. It should be noted that the high contribution rate of road-related sediment mainly reflected the situation that the highway is still under construction. In fact, with the road surface are harden and construction activities are completed, the road-related erosion would be reduced and so is the sediment that entering nearby channel [31]. Nevertheless, the high rate of sediment contributed by the road in this study still confirmed the suggestion of Wasson et al. (2022) [32], who reported that roads that cut across steep hillslopes in the Himalaya generate sediment that is usually deposited in rivers. Sediment deposition may lead to potential flood risks [35], aquatic environment hazards and endangerment of local ecosystems [34,36]. Therefore, more attention should be given to channel management and sediment generation, including roads erosion control, in disturbed watersheds. In order to mitigate soil erosion and sediment generation occurring on cutslopes and roadside slopes, vegetation restoration combined with soil stabilization measures such as the application of geotextiles and blankets could be employed [56]. Additionally, a well-designed road drainage system incorporating conservation measures, such as armored ditches and sediment pits, would help protect the roadbed from erosion [7]. During the process of sediment transport from roads to nearby channels, sediment basins, energy dissipation structures and in-channel grade control structures [57] may be beneficial in controlling channel erosion and reducing sediment transport to the main channel.

4.2. Mechanism of Spatial Variation in Sediment Contributed by Roads

The spatial variation in the sediment contributed by roads reflects the intensity of sediment generation and transport from roads. The four significant factors listed in Figures 6 and 7, that is, the channel gradient (CS), average road segment gradient (RS),

the ratio of the road length to the channel length (R/C), and the flow length between the sampling site and road (FL), could provide different perspectives for understanding the amounts of sediment contributed by roads. The significant positive correlation between the channel gradient (CS) and the rate of sediment contributed by the road could be explained by the sediment transport process within the channel above each sampling site. A higher channel gradient implies a higher transport capacity and sediment delivery ratio [36]. Therefore, more sediment from roads was transported downstream to the sampling site. Moreover, the positive correlation between the rate of sediment contributed by the road and the average road segment gradient (RS) reflected the erosion intensity on the road surface, which increased as the slope of the road segments increased. A relatively high erosion rate would in turn increase sediment transport to nearby channels. The linear equation between the rate of contributed sediment and slope of the road segment in Figure 7 was consistent with that of Cao et al. (2014, 2021) [58,59], in which the linear form of the road segment gradient could be used to describe the erosion rate of the road. The intercept of the linear function in the x-axis might imply that the critical slope gradient for road erosion to occur and affect rivers is approximately 3%.

The road segment length is another factor that determines the magnitude and intensity of road erosion, as reported by many studies [59–61]. This was confirmed by the relatively high importance of RL (0.148) in Figure 7. Nevertheless, the road length showed only a weak positive correlation with the rate of sediment contributed by the road segment. This might be because the road is parallel to the main channel; thus, road length is significantly related to channel length (R = 0.97), which is recognized as a critical influential factor for sediment deposition along channels [36]. The negative effect of channel length and the positive effect of road length might influence each other's correlation with the sediment contributed from the road. Notably, the ratio of the road length to the channel length (R/C) showed a significant correlation and importance, reflecting the combined effect of the sediment source of road erosion and sediment transport on the rate of sediment contributed by the road along the main channel. The linear function in Figure 7 shows an intercept close to 0.5 on the x-axis, which might imply that the sediment contributed by the road could be negligible when the road length is less than half of the channel length in the studied watershed.

In addition to the above road segment and channel terrain factors, the buffer area between roads and channels is also critical for sediment transport from roads [39]. Research has shown that the connection between a road network and a channel network is a key factor that determines the amount of sediment from a road that enters a channel [62]. The negative correlation between the FL (the flow length between the sampling site and the road) and SED implies that a shorter distance leads to a greater amount of sediment transported from the road to the downstream channel [63–66]. The highest values in Figure 7 illustrate that flow length is the most important factor affecting sediment contributed by roads. Notably, the FL had a greater correlation coefficient than the CRD, which represents the average distance between roads and channels. This means that the specific flow length is more important than the average buffer distance for determining the rate of sediment contributed by roads at a given sampling site. Nevertheless, the two factors are significantly correlated with each other (R = 0.75); therefore, the CRD also showed a high importance that was second only to that of the flow length. Figure 7 shows that the rate of sediment contributed by the road decreased logarithmically with increasing flow length. This finding is consistent with that of Cao et al. (2021) [7], who reported that sediment generation decreases logarithmically with increasing distance to roads. A critical distance of approximately 310 m could be calculated according to the intercept of the function with respect to the x-axis. This value is close to the maximum buffer length (300 m) suggested by Elliot et al. (1999) [67] in the WEPP:Road model, indicating the extent to which road erosion sediment affects adjacent rivers. This result might be meaningful for road route design in the study area and for guidance on maintaining safe distances from rivers. It should be noted that the above equations and critical values mainly represent the situation of the

studied watershed, where the road network structure is relatively simple. In the case of more complex road networks comprising different road grades, further research is required to elucidate the spatial variation mechanism of road-related sediment contribution. For example, the results of the fingerprint analysis could be related to the sediment connectivity that is altered by the intersection between the road network and the channel network. In addition, the spatiotemporal variations of sediment sources should also be taken into account when different constructions are carried out at different stages.

5. Conclusions

In this study, composite fingerprint analysis was conducted to explore the sources of deposited channel sediment in a road construction-disturbed tributary watershed of the YTRB. An optimum composite fingerprint combination of 10 factors, including Al_2O_3, TFe_2O_3, Sn, TP, Cr, Na_2O, Mn, W, SiO_2, and Sr, was established and indicated to accurately distinguish different sediment sources. According to the results of the multivariate mixed model, we found that the bank material contributed the most (52.52% on average) to the sediment deposited along the main channel. On the other hand, the forest and grassland hillslopes showed low erosion risk and accounted for 14.46% of the sediment. Roads, which occupied only 0.2% of the total area, contributed an average of 33.02% of the deposited channel sediment. These findings demonstrated that road construction disturbances have generated a nonnegligible sediment contribution despite their small areas within the watershed. The rate of sediment contributed by the road exhibited a large spatial variation along the channel, which was mainly affected by factors such as the flow length to the road, the slope of the road segment, the road segment length, and the ratio of the road segment length to the channel length. Among them, the flow length was found to be the most important factor. Therefore, maintaining a sufficient distance between roads and rivers should be a priority to prevent road sediment from entering channels and damaging aquatic environments. In addition, shortening the road segment length and reducing the gradient are critical for reducing sediment generation if the placement of roads close to rivers is inevitable.

Author Contributions: Conceptualization, L.C. and X.L.; methodology, X.L. and B.Z.; software, X.L. and R.L.; validation, B.Z. and R.L.; formal analysis, B.Z. and C.B.; investigation, B.Z. and R.L.; resources, L.C.; data curation, X.L. and B.Z.; writing—original draft preparation, X.L.; writing—review and editing, L.C.; visualization, X.L. and C.B.; supervision, L.C.; project administration, L.C. and X.W.; funding acquisition, L.C. and X.W. All authors have read and agreed to the published version of the manuscript.

Funding: This research was funded by the National Key Research and Development Program of China, grant number 2021YFB2600105, and the Natural Science Foundation of Sichuan Province, China, grant number 2024NSFSC0105.

Data Availability Statement: The data that support the findings of this study are available from the corresponding author upon reasonable request.

Acknowledgments: The authors would like to thank Mingming Shi and Junhao Li for their assistance with field sampling.

Conflicts of Interest: The authors declare no conflicts of interest.

References

1. Borrelli, P.; Robinson, D.A.; Fleischer, L.R.; Lugato, E.; Ballabio, C.; Alewell, C.; Meusburger, K.; Modugno, S.; Schütt, B.; Ferro, V.; et al. An assessment of the global impact of 21st century land use change on soil erosion. *Nat. Commun.* **2013**, *8*, 2013. [CrossRef]
2. Collins, A.L.; Walling, D.E.; Stroud, R.W.; Robson, M.; Peet, L.M. Assessing damaged road verges as a suspended sediment source in the Hampshire Avon catchment, southern United Kingdom. *Hydrol. Process.* **2010**, *24*, 1106–1122. [CrossRef]
3. Zhang, L.T.; Gao, Z.L.; Yang, S.W.; Li, Y.H.; Tian, H.W. Dynamic processes of soil erosion by runoff on engineered landforms derived from expressway construction: A case study of typical steep spoil heap. *Catena* **2015**, *128*, 108–121. [CrossRef]
4. Nosrati, K.; Collins, A.L.; Madankan, M. Fingerprinting sub-basin spatial sediment sources using different multivariate statistical techniques and the Modified MixSIR model. *Catena* **2018**, *164*, 32–43. [CrossRef]

5. Laurance, W.F.; Balmford, A. A global map for road building. *Nature* **2013**, *495*, 308–309. [CrossRef]
6. Jimenez, M.D.; Ruiz-Capillas, P.; Mola, I.; Pérez-Corona, E.; Casado, M.A.; Balaguer, L. Soil development at the roadside: A case study of a novel ecosystem. *Land Degrad. Dev.* **2013**, *24*, 564–574. [CrossRef]
7. Cao, L.X.; Elliot, W.; Long, J.W. Spatial simulation of forest road effects on hydrology and soil erosion after a wildfire. *Hydrol. Process.* **2021**, *35*, e14139. [CrossRef]
8. Gucinski, H.; Furniss, M.J.; Ziemer, R.R.; Brookes, M.H. *Forest Roads: A Synthesis of Scientific Information*; General Technical Report PNW-GTR-509; U.S. Dept. of Agriculture, Forest Service: Portland, OR, USA, 2001; p. 103.
9. Miller, M.E.; Elliot, W.J.; Billmire, M.; Robichaud, P.R.; Endsley, K.A. Rapid-response tools and datasets for post-fire remediation: Linking remote sensing and process-based hydrological models. *Int. J. Wildland Fire* **2016**, *25*, 1061–1073. [CrossRef]
10. Poesen, J. Soil erosion in the Anthropocene: Research needs. *Earth Surf. Process. Landf.* **2018**, *43*, 64–84. [CrossRef]
11. Krasa, J.; Dostal, T.; Jachymova, B.; Bauer, M.; Devaty, J. Soil erosion as a source of sediment and phosphorus in rivers and reservoirs—Watershed analyses using WaTEM/SEDEM. *Environ. Res.* **2019**, *171*, 470–483. [CrossRef] [PubMed]
12. Pant, N.; Dubey, R.K.; Bhatt, A.; Rai, S.P.; Semwal, P.; Mishra, S. Soil erosion and flood hazard zonation using morphometric and morphotectonic parameters in Upper Alaknanda river basin. *Nat. Hazards* **2020**, *103*, 3263–3301. [CrossRef]
13. Zhao, L.S.; Meng, P.; Zhang, J.S.; Zhang, J.X.; Li, J.X.; Wang, X.M. The contribution of human activities to runoff and sediment changes in the Mang River basin of the Loess Plateau, China. *Land Degrad. Dev.* **2023**, *34*, 28–41. [CrossRef]
14. Collins, A.L.; Pulley, S.; Foster, I.D.L.; Gellis, A.; Porto, P.; Horowitz, A.J. Sediment source fingerprinting as an aid to catchment management: A review of the current state of knowledge and a methodological decision-tree for end-users. *J. Environ. Manag.* **2017**, *194*, 86–108. [CrossRef]
15. Walling, D.E.; Owens, P.N.; Leeks, G.J.L. Fingerprinting suspended sediment sources in the catchment of the River Ouse, Yorkshire, UK. *Hydrol. Process.* **1999**, *13*, 955–975. [CrossRef]
16. Gaspar, L.; Blake, W.H.; Smith, H.G.; Lizaga, I.; Navas, A. Testing the sensitivity of a multivariate mixing model using geochemical fingerprints with artificial mixtures. *Geoderma* **2019**, *337*, 498–510. [CrossRef]
17. Pulley, S.; Foster, I.; Antunes, P. The application of sediment fingerprinting to floodplain and lake sediment cores: Assumptions and uncertainties evaluated through case studies in the Nene Basin, UK. *J. Soils Sediments* **2015**, *15*, 2132–2154. [CrossRef]
18. Gellis, A.C.; Sanisaca, L.G. Sediment Fingerprinting to Delineate Sources of Sediment in the Agricultural and Forested Smith Creek Watershed, Virginia, USA. *J. Am. Water Resour. Assoc.* **2018**, *54*, 1197–1221. [CrossRef]
19. Kemper, J.T.; Rathburn, S.L.; Friedman, J.M.; Nelson, J.M.; Mueller, E.R.; Vincent, K.R. Fingerprinting historical tributary contributions to floodplain sediment using bulk geochemistry. *Catena* **2022**, *214*, 106231. [CrossRef]
20. Fatahi, A.; Gholami, H.; Esmaeilpour, Y.; Fathabadi, A. Fingerprinting the spatial sources of fine-grained sediment deposited in the bed of the Mehran River, southern Iran. *Sci. Rep.* **2022**, *12*, 3880. [CrossRef]
21. Nosrati, K.; Haddadchi, A.; Collins, A.L.; Jalali, S.; Zare, M.R. Tracing sediment sources in a mountainous forest catchment under road construction in northern Iran: Comparison of Bayesian and frequentist approaches. *Environ. Sci. Pollut. Res.* **2018**, *25*, 30979–30997. [CrossRef] [PubMed]
22. Cheng, Q.Y.; Wang, S.J.; Peng, T.; Cao, L.; Zhang, X.B.; Buckerfield, S.J.; Zhang, Y.S.; Collins, A.L. Sediment sources, soil loss rates and sediment yields in a Karst plateau catchment in Southwest China. *Agric. Ecosyst. Environ.* **2020**, *304*, 107114. [CrossRef]
23. Huang, D.H.; Pei, M.Z.; Zhou, L.L.; Fan, H.M.; Jia, Y.F. Identification of sediment sources and exploration of scale effects in the black soil region of Northeast China. *Catena* **2020**, *195*, 104848. [CrossRef]
24. Shi, Z.L.; Blake, W.H.; Wen, A.B.; Chen, J.C.; Yan, D.C.; Long, Y. Channel erosion dominates sediment sources in an agricultural catchment in the Upper Yangtze basin of China: Evidence from geochemical fingerprints. *Catena* **2021**, *199*, 105111. [CrossRef]
25. Tian, P.; An, Z.F.; Zhao, G.J.; Gao, P.; Li, P.F.; Sun, W.Y.; Mu, X.M. Assessing sediment yield and sources using fingerprinting method in a representative catchment of the Loess Plateau, China. *Environ. Earth Sci.* **2019**, *78*, 261. [CrossRef]
26. Guo, Q.K.; Shan, Z.J.; Lu, W.; Qin, W.; Yin, Z.; Xu, H.C. Fingerprinting sediment sources in two typical watersheds in the dry-hot valleys of Southwest China: The role of gully and orchard land. *Catena* **2023**, *233*, 107479. [CrossRef]
27. Motha, J.A.; Wallbrink, P.J.; Hairsine, P.B.; Grayson, R.B. Unsealed roads as suspended sediment sources in an agricultural catchment in south-eastern Australia. *J. Hydrol.* **2004**, *286*, 1–18. [CrossRef]
28. Nosrati, K.; Collins, A.L. Investigating the importance of recreational roads as a sediment source in a mountainous catchment using a fingerprinting procedure with different multivariate statistical techniques and a Bayesian un-mixing model. *J. Hydrol.* **2019**, *569*, 506–518. [CrossRef]
29. Nematollahi, S.; Fakheran, S.; Soffianian, A. Ecological impact assessment of road networks at landscape scale using spatial road disturbance index (SPROADI). *J. Environ. Eng. Landsc. Manag.* **2017**, *25*, 297–304. [CrossRef]
30. Zhao, Y.; Zhang, F.; Zeng, C.; Shi, X.A.; Kong, J.Y.; Xie, S.Q. Quantifying the sources of suspended sediments in the Nianchu River Basin, southern Tibetan Plateau: Evaluation and application of a semiempirical fingerprinting framework. *J. Hydrol.* **2024**, *630*, 130711. [CrossRef]
31. Huang, Z.; Lin, B.L.; Sun, J.; Nima, L.Z.; Da, P.; Dawa, J.M. Suspended Sediment Transport Responses to Increasing Human Activities in a High-Altitude River: A Case Study in a Typical Sub-Catchment of the Yarlung Tsangpo River. *Water* **2020**, *12*, 952. [CrossRef]

32. Wasson, R.; Acharjee, S.; Rakshit, R. Towards identification of sediment sources, and processes of sediment production, in the Yarlung-Tsangpo-Brahmaputra River catchment for reduction of fluvial sediment loads. *Earth-Sci. Rev.* **2022**, *226*, 103932. [CrossRef]
33. Shi, X.N.; Zhang, F.; Lu, X.X.; Wang, Z.Y.; Gong, T.L.; Wang, G.X.; Zhang, H.B. Spatiotemporal variations of suspended sediment transport in the upstream and midstream of the Yarlung Tsangpo River (the upper Brahmaputra), China. *Earth Surf. Process. Landf.* **2018**, *43*, 432–443. [CrossRef]
34. Li, J.L.; Wang, G.X.; Song, C.L.; Sun, S.Q.; Ma, J.P.; Wang, Y.; Guo, L.M.; Li, D.F. Recent intensified erosion and massive sediment deposition in Tibetan Plateau rivers. *Nat. Commun.* **2024**, *15*, 722. [CrossRef] [PubMed]
35. Chen, S.; Zhu, S.C.; Wen, X.; Shao, H.Y.; He, C.J.; Qi, J.G.; Lv, L.F.; Han, L.B.; Liu, S.H. Mapping Potential Soil Water Erosion and Flood Hazard Zones in the Yarlung Tsangpo River Basin, China. *Atmosphere* **2023**, *14*, 49. [CrossRef]
36. Chen, H.S.; Lan, L.; Nie, Y.P.; Wang, Y.G.; Wang, X.K. Assessment of sediment transport in Luxiapuqu watershed using RUSLE-TLSD and InSAR techniques: Yarlung Tsangpo River, China. *Environ. Sci. Pollut. Res.* **2024**, *31*, 8082–8098. [CrossRef]
37. Teng, H.F.; Liang, Z.Z.; Chen, S.C.; Liu, Y.; Rossel, R.A.V.; Chappell, A.; Yu, W.; Shi, Z. Current and future assessments of soil erosion by water on the Tibetan Plateau based on RUSLE and CMIP5 climate models. *Sci. Total Environ.* **2018**, *635*, 673–686. [CrossRef] [PubMed]
38. Bravo-Linares, C.; Ovando-Fuentealba, L.; Muñoz-Arcos, E.; Kitch, J.L.; Millward, G.E.; López-Gajardo, R.; Cañoles-Zambrano, M.; Del Valle, A.; Kelly, C.; Blake, W.H. Basin scale sources of siltation in a contaminated hydropower reservoir. *Sci. Total Environ.* **2024**, *914*, 169952. [CrossRef] [PubMed]
39. Elliot, W.J. WEPP internet interfaces for forest erosion prediction. *J. Am. Water Resour. Assoc.* **2004**, *40*, 299–309. [CrossRef]
40. Laceby, J.P.; Evrard, O.; Smith, H.G.; Blake, W.H.; Olley, J.M.; Minella, J.P.G.; Owens, P.N. The challenges and opportunities of addressing particle size effects in sediment source fingerprinting: A review. *Earth-Sci. Rev.* **2017**, *169*, 85–103. [CrossRef]
41. Li, X.; Shi, M.M.; Cao, L.X.; Chen, G.; Wang, Y.; Yao, L.F. A composite fingerprinting analysis of sediment sources in a construction-disturbed small watersheds of Southeast Tibet. *Sci. Soil Water Conserv.* **2023**, *21*, 113–122. [CrossRef]
42. Wilkinson, S.N.; Hancock, G.J.; Bartley, R.; Hawdon, A.A.; Keen, R.J. Using sediment tracing to assess processes and spatial patterns of erosion in grazed rangelands, Burdekin River basin, Australia. *Agric. Ecosyst. Environ.* **2013**, *180*, 90–102. [CrossRef]
43. Collins, A.L.; Walling, D.E.; Leeks, G.J.L. Source type ascription for fluvial suspended sediment based on a quantitative composite fingerprinting technique. *Catena* **1997**, *29*, 1–27. [CrossRef]
44. Franz, C.; Makeschin, F.; Weiss, H.; Lorz, C. Sediments in urban river basins: Identification of sediment sources within the Lago Paranoa catchment, Brasilia DF, Brazil—Using the fingerprint approach. *Sci. Total Environ.* **2014**, *466*, 513–523. [CrossRef]
45. Minella, J.P.G.; Walling, D.E.; Merten, G.H. Combining sediment source tracing techniques with traditional monitoring to assess the impact of improved land management on catchment sediment yields. *J. Hydrol.* **2008**, *348*, 546–563. [CrossRef]
46. Walling, D.E. Tracing suspended sediment sources in catchments and river systems. *Sci. Total Environ.* **2005**, *344*, 159–184. [CrossRef] [PubMed]
47. Liaw, A.; Wiener, M. Classification and regression by randomForest. *R News* **2002**, *2*, 18–22.
48. Thomaz, E.L.; Vestena, L.R.; Scharrón, C.E.R. The effects of unpaved roads on suspended sediment concentration at varying spatial scales—A case study from Southern Brazil. *Water Environ. J.* **2014**, *28*, 547–555. [CrossRef]
49. Farias, T.R.L.; Medeiros, P.H.A.; de Araújo, J.C.; Navarro-Hevia, J. The role of unpaved roads in the sediment budget of a semiarid mesoscale catchment. *Land Degrad. Dev.* **2021**, *32*, 5443–5454. [CrossRef]
50. Cao, L.X.; Zhang, K.L.; Dai, H.L.; Liang, Y. Modeling Interrill Erosion on Unpaved Roads in the Loess Plateau of China. *Land Degrad. Dev.* **2015**, *26*, 825–832. [CrossRef]
51. Zhang, Y.; Zhao, Y.Y.; Liu, B.Y.; Wang, Z.Q.; Zhang, S. Rill and gully erosion on unpaved roads under heavy rainfall in agricultural watersheds on China's Loess Plateau. *Agric. Ecosyst. Environ.* **2019**, *284*, 106580. [CrossRef]
52. Cao, L.X.; Zhang, K.L.; Zhang, W. Detachment of road surface soil by flowing water. *Catena* **2009**, *76*, 155–162. [CrossRef]
53. Negishi, J.N.; Sidle, R.C.; Ziegler, A.D.; Noguchi, S.; Rahim, N.A. Contribution of intercepted subsurface flow to road runoff and sediment transport in a logging-disturbed tropical catchment. *Earth Surf. Process. Landf.* **2008**, *33*, 1174–1191. [CrossRef]
54. Shu, C.B.; Liu, G.; Zhang, Q.; Xu, J.H.; Chen, H.; Dan, C.X.; Wang, X.K.; Shen, Y.L.; Liu, Y.; Guo, Z.; et al. Fingerprinting sediment sources in mountainous catchments disturbed by plantation and construction activities in southern China. *Land Degrad. Dev.* **2024**, *35*, 3287–3301. [CrossRef]
55. Zhao, Q.H.; Jing, Y.R.; Wang, A.; Yu, Z.H.; Liu, Y.; Yu, J.H.; Liu, G.S.; Ding, S.Y. Response of Sediment Connectivity to Altered Convergence Processes Induced by Forest Roads in Mountainous Watershed. *Remote Sens.* **2022**, *14*, 3603. [CrossRef]
56. Ramos-Scharrón, C.E.; Alicea-Díaz, E.E.; Figueroa-Sánchez, Y.A.; Viqueira-Ríos, R. Road cutslope erosion and control treatments in an actively-cultivated tropical montane setting. *Catena* **2022**, *209*, 105814. [CrossRef]
57. Robichaud, P.R.; Storrar, K.A.; Wagenbrenner, J.W. Effectiveness of straw bale check dams at reducing post-fire sediment yields from steep ephemeral channels. *Sci. Total Environ.* **2019**, *676*, 721–731. [CrossRef] [PubMed]
58. Cao, L.X.; Zhang, K.L.; Liang, Y. Factors affecting rill erosion of unpaved loess roads in China. *Earth Surf. Process. Landf.* **2014**, *39*, 1812–1821. [CrossRef]
59. Cao, L.X.; Wang, Y.; Liu, C. Study of unpaved road surface erosion based on terrestrial laser scanning. *Catena* **2021**, *199*, 105091. [CrossRef]

60. Luce, C.H.; Black, T.A. Sediment production from forest roads in western Oregon. *Water Resour. Res.* **1999**, *35*, 2561–2570. [CrossRef]
61. MacDonald, L.H.; Sampson, R.W.; Anderson, D.M. Runoff and road erosion at the plot and road segment scales, St John, US Virgin Islands. *Earth Surf. Process. Landf.* **2001**, *26*, 251–272. [CrossRef]
62. Sosa-Pérez, G.; MacDonald, L. Wildfire effects on road surface erosion, deposition, and road-stream connectivity. *Earth Surf. Process. Landf.* **2017**, *42*, 735–748. [CrossRef]
63. Parsakhoo, A.; Lotfalian, M.; Kavian, A.; Hosseini, S.A. Prediction of the soil erosion in a forest and sediment yield from road network through GIS and SEDMODL. *Int. J. Sediment Res.* **2014**, *29*, 118–125. [CrossRef]
64. Benda, L.; James, C.; Miller, D.; Andras, K. Road Erosion and Delivery Index (READI): A Model for Evaluating Unpaved Road Erosion and Stream Sediment Delivery. *J. Am. Water Resour. Assoc.* **2019**, *55*, 459–484. [CrossRef]
65. Dangle, C.L.; Bolding, M.C.; Aust, W.M.; Barrett, S.M.; Schilling, E.B. Best Management Practices Influence Modeled Erosion Rates at Forest Haul Road Stream Crossings in Virginia. *J. Am. Water Resour. Assoc.* **2019**, *55*, 1169–1182. [CrossRef]
66. Ramos-Scharrón, C.E. Impacts of off-road vehicle tracks on runoff, erosion and sediment delivery—A combined field and modeling approach. *Environ. Modell. Softw.* **2021**, *136*, 104957. [CrossRef]
67. Elliot, W.J.; Hall, D.E.; Scheele, D.L. *WEPP Interface for Predicting Forest Road Runoff, Erosion and Sediment Delivery*; Technical Documentation; U.S.D.A. Forest Service Rocky Mountain Research Station: Moscow, ID, USA. Available online: http://forest.moscowfsl.wsu.edu/fswepp/docs/wepproaddoc.html (accessed on 2 May 2024).

Disclaimer/Publisher's Note: The statements, opinions and data contained in all publications are solely those of the individual author(s) and contributor(s) and not of MDPI and/or the editor(s). MDPI and/or the editor(s) disclaim responsibility for any injury to people or property resulting from any ideas, methods, instructions or products referred to in the content.